

Towards More Practical Group Activity Detection: A New Benchmark and Model

Dongkeun Kim¹ Youngkil Song² Minsu Cho^{1,2} Suha Kwak^{1,2}
Department of CSE, POSTECH¹ Graduate School of AI, POSTECH²

<https://cvlab.postech.ac.kr/research/CAFE>

Abstract

Group activity detection (GAD) is the task of identifying members of each group and classifying the activity of the group at the same time in a video. While GAD has been studied recently, there is still much room for improvement in both dataset and methodology due to their limited capability to address practical GAD scenarios. To resolve these issues, we first present a new dataset, dubbed Café. Unlike existing datasets, Café is constructed primarily for GAD and presents more practical evaluation scenarios and metrics, as well as being large-scale and providing rich annotations. Along with the dataset, we propose a new GAD model that deals with an unknown number of groups and latent group members efficiently and effectively. We evaluated our model on three datasets including Café, where it outperformed previous work in terms of both accuracy and inference speed. Both our dataset and code base will be open to the public to promote future research on GAD.

1. Introduction

Understanding group activities in videos plays a crucial role in numerous applications such as visual surveillance, social scene understanding, and sports analytics. The generic task of group activity understanding is complex and challenging since it involves identifying participants in an activity and perceiving their spatio-temporal relations as well as recognizing actions of individual actors. Due to these difficulties, most existing work on group activity understanding has been limited to the task of categorizing an entire video clip into one of predefined activity classes [1, 15, 23, 29, 35, 45, 50], which is called the group activity recognition (GAR) in the literature. The common setting of GAR assumes that only a single group activity appears per clip and actors taking part of the activity are identified manually in advance. However, these assumptions do not hold in many real crowd videos, which often exhibit multiple groups that perform their own activities and *outliers* who do not belong

to any group. Moreover, it is impractical to manually identify the actors relevant to each group activity in advance. Hence, although GAR has served as a representative group activity understanding task for a decade, its practical value is largely limited.

As a step toward more realistic group activity understanding, group activity detection (GAD), also known as social activity recognition, has recently been studied [11, 12, 41]. GAD aims to localize multiple groups in a video clip and classify each of the localized groups into one of predefined group activity classes, where the group localization means identifying actors of each group given bounding boxes of the actors. Although a few prior work sheds light on this new and challenging task, there is still large room for improvement in both dataset and methodology due to their limited capability to address practical GAD scenarios. Existing datasets for GAD [11, 12] are not constructed primarily for the task but are extensions of other datasets [5, 32] with additional group labels. Moreover, most of the groups in these datasets are singletons, which are individuals rather than groups. Meanwhile, most GAD models localize groups using off-the-shelf clustering algorithms, which are not only too heavy in computation but also not optimized for the task.

To address the dataset issue, we present a new dataset for GAD, dubbed Café. Qualitative examples of videos in Café are presented in Fig. 1. The videos were taken at six different cafes to capture realistic daily activities, and each of them exhibits multiple non-singleton groups performing their own activities as well as outliers, presenting more practical evaluation scenarios for GAD. Café has two more advantages over the existing GAD datasets. First, its scale is substantially larger as it provides 10K clips and 3.5M actor bounding box labels as summarized in Table 1. Second, in Café, the same scene is captured by at most four cameras with different viewpoints; these multi-view videos can be used to evaluate model’s generalization performance on unseen views as well as unseen places.

In addition to the new dataset, we also propose a new model architecture for end-to-end GAD. Our model builds

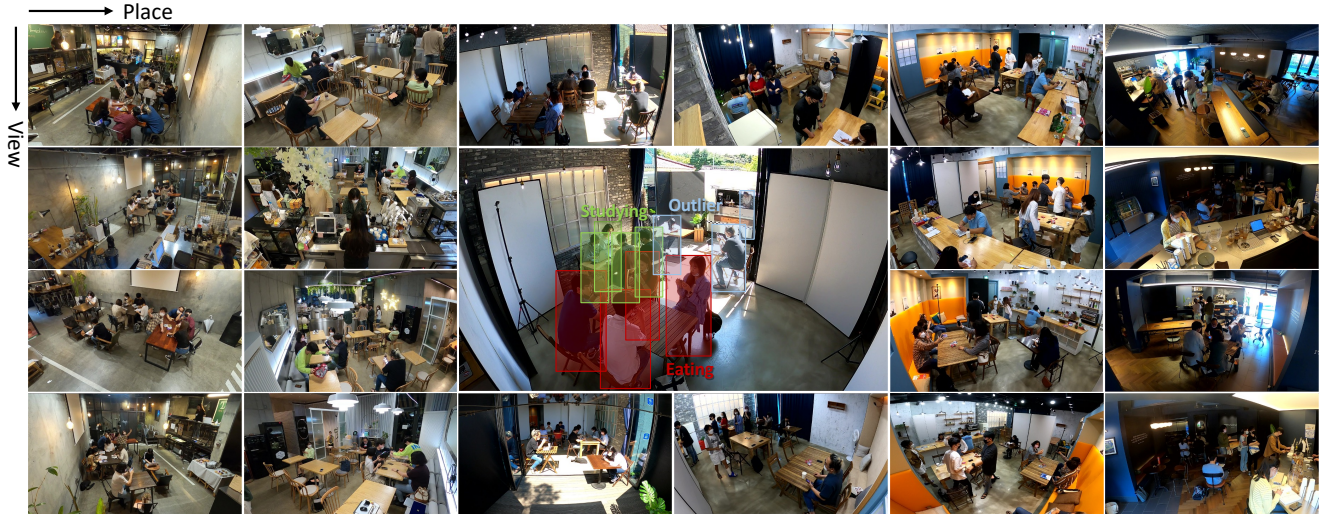


Figure 1. Examples of videos in Café. The videos were taken at six different places and four cameras with different viewpoints.

Dataset	# Clips	Resolution	# Boxes	Source	Multi-group	Multi-view
CAD [5]	2,511	720 × 480	0.1M	Daily videos	✗	✗
Volleyball [22]	4,830	1280 × 720	1.2M	Sports videos	✗	✗
NBA [48]	9,172	1280 × 720	-	Sports videos	✗	✗
PLPS [37]	71	1920 × 1080	0.2M	Daily videos	✓	✗
Social-CAD [11]	2,511	720 × 480	0.1M	Daily videos	✓	✗
JRDB-Act [12]	3,625	3760 × 480	2.5M	Daily videos	✓	✗
Café	10,297	1920 × 1080	3.5M	Daily videos	✓	✓

Table 1. Comparison between Café and other datasets for group activity understanding.

embedding vectors of group candidates and individual actors through the attention mechanism of Transformer [10, 42]. Unlike GAR approaches using Transformer, which aggregate actor features to form a single group representation while capturing spatio-temporal relationship between actors, our model divides actors into multiple groups, each with its own group representation. Embedding vectors of an actor and a group are learned to be close to each other if the actor is a member of the group so that group localization is done by matching the actor and group embeddings. To deal with an unknown number of groups, we deploy learnable group tokens whose number is supposed to be larger than the possible maximum number of groups in a video clip; the tokens are then transformed into group embeddings by Transformer attending to actor embeddings. Each group embedding is also used as input to the activity classifier that determines its activity class. This mechanism allows to discover groups accurately without off-the-shelf clustering algorithms unlike most of previous work, leading to substantially faster inference.

We evaluated our model on three datasets, Café, Social-CAD [11], and JRDB-Act [12], where it outperformed previous work in terms of both accuracy and inference speed.

In summary, our contribution is three-fold as follows:

- We introduce Café, a new large-scale dataset for GAD. Thanks to its large-scale and rich annotations, it can serve as a challenging benchmark for GAD.
- We present a new GAD model based on Transformer to deal with an unknown number of groups and latent group members without off-the-shelf clustering algorithms.
- Our model outperformed previous work on Café and two other GAD benchmarks in terms of both GAD accuracy and inference speed.

2. Related Work

2.1. Group Activity Recognition

Group activity recognition (GAR) has been extensively studied as a representative group activity understanding task. With the advent of deep learning, recurrent neural networks have substantially improved GAR performance [2, 9, 21, 22, 31, 36, 40, 44, 46]. In particular, hierarchical long short-term memory networks [21, 44, 46] have been used to model the dynamics of individual actors and aggregate actors to infer the dynamics of a group.

A recent trend in GAR is to model spatio-temporal relations between actors. To this end, modules for modeling such relations, such as graph neural networks (GNN) [11, 20, 45, 47, 50], have been placed on top of a convolutional neural network. Popular examples of such modules include graph convolutional networks [45], graph attention networks [11], and dynamic relation graphs [50]. To employ global spatio-temporal dynamic relations between actors and contexts, Transformers [10, 42] have been adopted for GAR and shown significant performance improvement [15, 23, 29, 30, 35, 49]. They utilize the attention mechanism to employ spatio-temporal actor relations [15, 30], relational contexts with conditional random fields [35], actor-specific scene context [49], intra- and inter-group contexts [29], and partial contexts of a group activity [23]. Although these methods have demonstrated outstanding performance, since GAR assumes that only one group is present in each video, their applicability in real-world scenarios is substantially limited.

2.2. Group Activity Detection

Group activity detection (GAD) has recently been studied to address the limitation of GAR. GNNs [11, 12] have been utilized to model relations between actors and divide actors into multiple groups by applying graph spectral clustering [33, 51]. However, they require off-the-shelf clustering algorithms, which are not optimized for the task and resulting slow inference speed. Meanwhile, HGC [41], which is most relevant to our work, adopts Deformable DETR [54] for group localization and matches a group and its potential members in 2D coordinate space. Unlike HGC, our model conducts such a matching in an embedding space to exploit semantic clues more explicitly, achieving better performance.

Along with these models, two datasets have been proposed. Social-CAD [11] has been constructed by extending an existing GAR dataset dubbed CAD [5] with additional sub-group labels. On the other hand, JRDB-Act [12] has extended annotations of JRDB [32], which is a dataset captured by a mobile robot with panoramic views. On both datasets, actors are divided into multiple groups, and the activity of each group is determined by majority voting of individual actions. However, most of the groups in these datasets are composed of a single actor, which is an individual who does not interact with other actors. Unlike these datasets, Café is constructed primarily for GAD. Also, in Café, people annotated as a group perform an activity together, and singleton groups are annotated as outliers.

3. Café Dataset

Café is a multi-person video dataset that aims to introduce a new challenging benchmark for GAD. The dataset contains more than 4 hours of videos taken at six different

cafes by four cameras with different viewpoints, and provides rich annotations including 3.5M bounding boxes of humans, their track IDs, group configurations, and group activity labels. Each of the videos is segmented into 6-second clips, and in each clip, each actor is a member of a group that performs one of six different group activities or is an *outlier* who does not belong to any group (*i.e.*, a singleton group). Also, outliers are often located overly close to groups as shown in Fig. 1. Thus, for group localization in Café, it is required to grasp the properties of individual actors and their semantic relations as well as their spatial proximity.

3.1. Data Annotation

Human annotators selected the key frame that exhibits group activities most clearly for each clip, and then annotated actor bounding boxes, group configurations, and group activity label per group in the frame. Next, a multi-object tracker [53] was applied to the clips to extend the actor box labels of the key frames to actor tracklets across frames. To improve the quality of estimated tracklets, the tracker incorporated a person detector [16] pre-trained on public datasets for person detection and tracking such as CrowdHuman [39], MOT17 [7], City Person [52], and ETHZ [13], and then finetuned on the key frames of Café. Finally, the human annotators manually fixed incorrect tracking IDs and bounding box coordinates. Since Café also provides human bounding boxes and their track IDs, it can also be used as a benchmark for multi-object tracking.

3.2. Dataset Splitting

To examine both place and viewpoint generalization of tested models, we split the dataset in two different ways: *split by view* and *split by place*. For the *split by view* setting, 4 videos of each place are split into 2 training, 1 validation, and 1 test videos. In a total of 6 places, 24 videos are split into 12 training, 6 validation, and 6 test videos. On the other hand, for the *split by place* setting, 24 videos are split into 16 training videos of 4 places, 4 validation videos of 1 place, and 4 test videos of 1 place.

3.3. Dataset Statistics

Important statistics that characterize Café are summarized in Fig. 2. Fig. 2a shows group population versus group size (*i.e.*, the number of group members) for each activity class. The class distribution of Café is imbalanced: The least frequent group activity *Queueing* appears about seven times fewer than the most frequent group activity *Taking Selfie*. Such an imbalance is natural in the real world, and may deteriorate activity classification accuracy.

As shown in Fig. 2b, the number of actors in each video clip varies from 3 to 14, and most clips contain 10 or 11 actors. We thus argue that videos in Café well simulate real

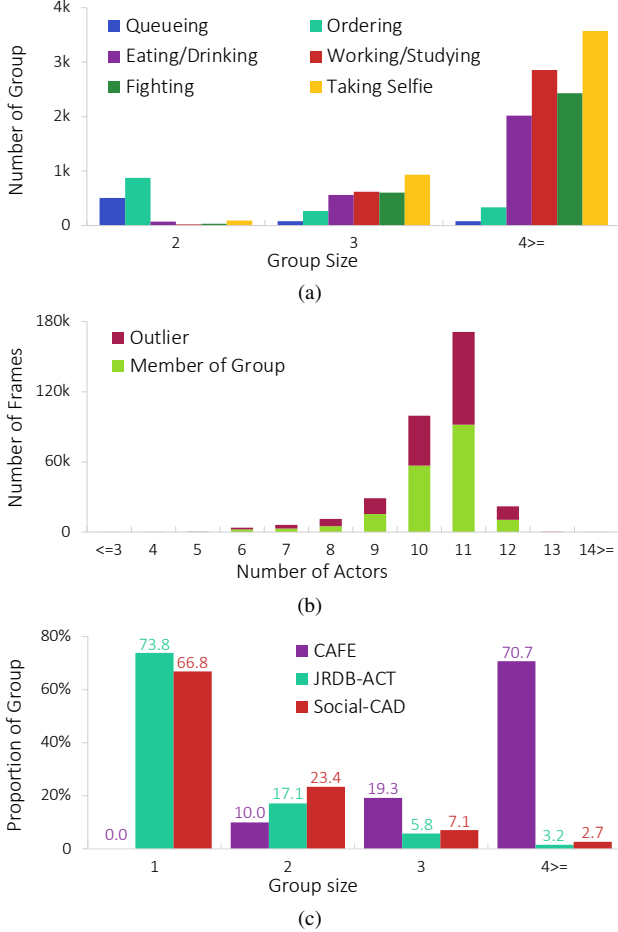


Figure 2. A summary of statistics of Café. (a) Group population versus group size per activity class. (b) Distribution of the number of actors in each video frame. (c) Comparison between Café and the other datasets in terms of group size.

crowd scenes. Also, it turns out that about half of the actors are outliers in each clip, which suggests that, on Café, group localization is more challenging.

Finally, Fig. 2c compares Café and the other two GAD datasets, Social-CAD and JRDB-Act, in terms of group size. Most groups of these datasets comprise only a single actor, which are not actually groups but individuals. On the other hand, all groups in Café have at least two actors, and mostly contain more than four actors.

3.4. Evaluation Metrics

A proper evaluation metric for GAD should consider following two aspects of predictions: (1) group localization, *i.e.*, identification of members per group, and (2) activity classification per group. While a few evaluation metrics such as social accuracy, social mAP, and G-Act mAP were already proposed in previous work [11, 12], they evaluate group localization based on individual actors rather than

groups, which makes them less strict criterion for evaluating group localization quality.

Hence, we propose new evaluation metrics for GAD: *Group mAP* and *Outlier mIoU*. *Group mAP* is a modification of mAP that has been widely used as the standard performance metric for object detection. On the other hand, *Outlier mIoU* evaluates how much correctly a model identifies outliers of input video.

Group mAP. Before introducing the definition of *Group mAP*, we first define *Group IoU*, which is proposed in previous work [6], analogous to IoU used in computation of mAP for object detection. *Group IoU* measures group localization accuracy by comparing a ground-truth group and a predicted group as follows:

$$\text{Group IoU}(G, \hat{G}) = \frac{|G \cap \hat{G}|}{|G \cup \hat{G}|}, \quad (1)$$

where G is a ground-truth group and \hat{G} is a predicted group; both groups are sets of actors. *Group IoU* is 1 if all members of \hat{G} are exactly the same with those of G and 0 if no member co-occurs between them. \hat{G} is considered as a correctly localized group if there exists a ground-truth group G that holds $\text{Group IoU}(G, \hat{G}) \geq \theta$, where θ is a predefined threshold. Note that we use two thresholds, $\theta = 1.0$ and $\theta = 0.5$, for evaluation. *Group mAP* is then defined by using *Group IoU* as a localization criterion along with activity classification scores. To be specific, we utilize the classification score of the ground-truth activity class as the detection confidence score of the predicted group, and calculate average precision (AP) score per activity class through all-point interpolation [14]. Finally, AP scores of all classes are averaged to produce *Group mAP*.

Outlier mIoU. It is important for GAD in the real world videos to distinguish groups and outliers (*i.e.*, singletons). We thus propose *Outlier mIoU* to evaluate outlier detection. Similar to *Group IoU*, its format definition is given by

$$\text{Outlier mIoU} = \frac{1}{|V|} \sum_{v \in V} \frac{|O_v \cap \hat{O}_v|}{|O_v \cup \hat{O}_v|}, \quad (2)$$

where $|V|$ is the set of video clips for evaluation, O_v is the set of ground-truth outliers in clip v , and \hat{O}_v is the set of predicted outliers in clip v .

4. Proposed Model for GAD

The purpose of GAD is to identify members of each group (*i.e.*, group localization) and classify the activity conducted by each group simultaneously. The task is challenging since both the number of groups and their members are unknown. We present a new model based on Transformer [10, 42] to deal with these difficulties; its overall architecture is illustrated in Fig. 3.

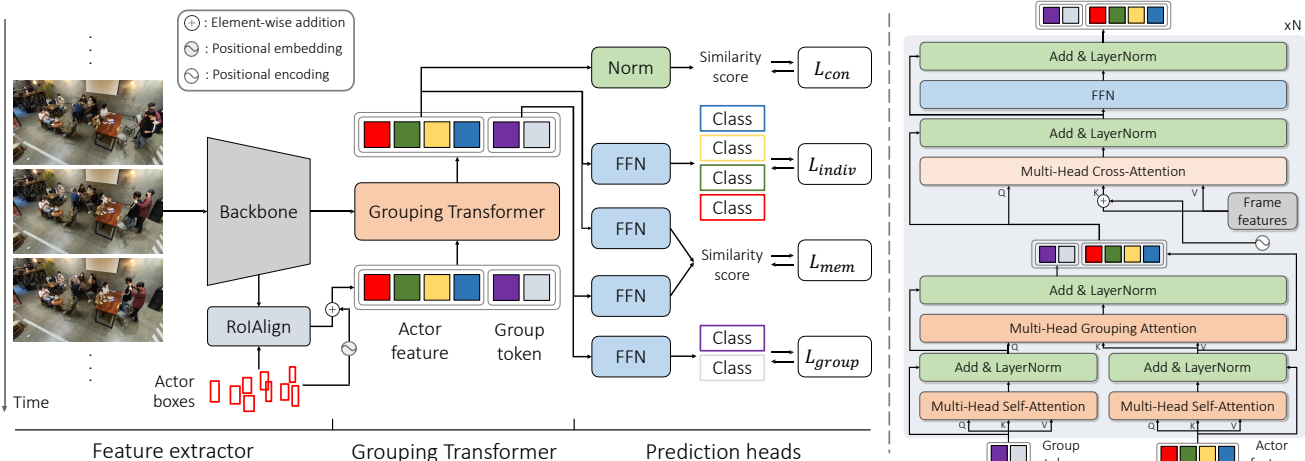


Figure 3. (Left) Overall architecture of our model. (Right) Detailed architecture of the Grouping Transformer.

The key idea at the heart of our model is that embedding vectors of an actor and a group should be close if the actor is a member of the group. To compute embedding vectors of groups and individual actors, we adopt attention mechanism of Transformer. To deal with a varying number of groups in each video clip, our model defines and utilizes learnable group tokens, whose number is supposed to be larger than the possible maximum number of groups in a clip. The group tokens along with actor features obtained by RoIAlign [19] are fed to a Transformer called Grouping Transformer to become the embedding vectors.

The rest of this section elaborates on the architecture and training objectives of our model.

4.1. Model Architecture

Our model consists of three parts: feature extractor, Grouping Transformer, and prediction heads.

Feature extractor. As in recent GAR models [11, 12, 15, 29, 45, 49], our model extracts frame-level features using a convolutional neural network, and extracts actor features from the frame features by RoIAlign given actor bounding boxes. To be specific, we adopt an ImageNet [8] pretrained ResNet-18 [18] for the feature extraction, and actor features extracted by RoIAlign are of 5×5 size. Additionally, to incorporate spatial cues when identifying group members, learnable positional embeddings of actor box coordinates are added to their associated actor features.

Grouping Transformer. Grouping Transformer takes learnable group tokens, actor features, and frame features as input, and produces embedding vectors of group candidates and actors in a frame-wise manner. As illustrated in the right-hand side of Fig. 3, it comprises three types of multi-head attention layers: (1) multi-head self-attention layers that capture relations between actors and those between groups separately, (2) multi-head grouping attention layers

where group tokens as queries attend to actor features serving as keys and values, and (3) multi-head cross-attention layers where actor features and group tokens draw attentions on frame features to capture contextual information. The core of the Grouping Transformer lies in the grouping attention layer. Each group token produces group representation by attending to actor features potentially belonging to its group, based on the similarity in the embedding space. In addition, to exploit spatial cues, we apply a distance mask to the multi-head self-attention layers for actor features: Following ARG [45], a pair of actors whose distance is greater than a threshold μ do not attend to each other.

Prediction heads. Two types of prediction heads in the form of feed-forward networks (FFNs) are attached to individual outputs of the Grouping Transformer, actor embeddings and group embeddings. The first prediction heads are for group activity classification, and the second prediction heads further project the actor/group embeddings so that the results are used for identifying group members: An actor embedding and a group embedding projected separately are dot-producted to compute their semantic affinity, which is used as the membership score of the actor for the group. At inference, each actor is assigned to the group with the highest membership score among all predicted groups.

4.2. Training Objectives

Group matching loss. Motivated by DETR [3], we first establish the optimal bipartite matching between ground-truth groups and predicted groups using Hungarian algorithm [26]. Since our model produces K predicted groups, where K is the number of group tokens and is supposed to be larger than the number of ground-truth groups, we add empty groups with no activity class, denoted by \emptyset , to the set of ground-truth groups so that the number of ground-truth groups becomes K and they are matched with the predicted

groups in a bipartite manner accordingly. Then, among all possible permutations of K predicted groups, denoted by \mathfrak{S}_K , Hungarian algorithm finds the permutation with the lowest total matching cost:

$$\hat{\sigma} = \arg \min_{\sigma \in \mathfrak{S}_K} \sum_i^K C_{i, \sigma(i)}. \quad (3)$$

$C_{i, \sigma(i)}$ in Eq. (3) is the matching cost of the ground-truth group i and the predicted group $\sigma(i)$ and is given by

$$C_{i, \sigma(i)} = -\mathbb{1}_{\{y_i \neq \emptyset\}} \hat{p}_{\sigma(i)}(y_i) + \mathbb{1}_{\{y_i \neq \emptyset\}} \|\mathbf{m}_i - \hat{\mathbf{m}}_{\sigma(i)}\|_2, \quad (4)$$

where y_i is the activity class label of the ground-truth group i and $\hat{p}_{\sigma(i)}(y_i)$ is the predicted class probability for y_i . Also, $\mathbf{m}_i = [m_i^1, \dots, m_i^N]^T$ indicates ground-truth membership relations between actors and group i , and $\hat{\mathbf{m}}_{\sigma(i)} = [\hat{m}_{\sigma(i)}^1, \dots, \hat{m}_{\sigma(i)}^N]^T$ is a collection of predicted membership scores of actors for predicted group $\sigma(i)$, where N is the number of actors in the input clip; each dimension of the two vectors is computed by

$$m_i^j = \begin{cases} 1, & \text{if actor } j \text{ is a member of group } i, \\ 0, & \text{otherwise,} \end{cases} \quad (5)$$

$$\hat{m}_{\sigma(i)}^j = \psi_j^T \phi_{\sigma(i)}, \quad (6)$$

where ψ_j is the output of the second prediction head for actor j and $\phi_{\sigma(i)}$ is the output of the second prediction head for predicted group $\sigma(i)$. The group activity classification loss L_{group} and the membership loss L_{mem} are calculated for all matched pairs. To be specific, we adopt the standard cross-entropy loss for $L_{\text{group}} = L_{\text{group}}(i, \sigma(i))$:

$$L_{\text{group}} = -\log \frac{\exp(\hat{p}_{\sigma(i)}(y_i))}{\sum_{c=1}^C \exp(\hat{p}_{\sigma(i)}(c))}, \quad (7)$$

where C is the number of group activity classes, and the binary cross-entropy loss for $L_{\text{mem}} = L_{\text{mem}}(i, \sigma(i))$:

$$L_{\text{mem}} = -\frac{1}{N} \sum_{j=1}^N (m_i^j \cdot \log \hat{m}_{\sigma(i)}^j + (1 - m_i^j) \cdot \log(1 - \hat{m}_{\sigma(i)}^j)). \quad (8)$$

Group consistency loss. It has been known that supervisory signals given by the bipartite matching of Hungarian algorithm may fluctuate and thus lead to slow convergence [27]. To alleviate this issue, we additionally introduce a group consistency loss, which is a modification of InfoNCE [34] and enhances the quality of group localization while bypassing the bipartite matching. The loss is formulated by

$$L_{\text{con}} = -\sum_{g_i} \sum_{j \in g_i} \log \frac{\sum_{k \in g_i, k \neq j} \exp(\cos(f_j, f_k)/\tau)}{\sum_{k \neq j} \exp(\cos(f_j, f_k)/\tau)}, \quad (9)$$

where g_i means the i -th ground-truth group, τ is the temperature, f_j stands for j -th actor embeddings and \cos indicates the cosine similarity function. This loss provides a consistent group information to actor embeddings that belong to the same group.

Individual action classification loss. We adopt a standard cross-entropy loss for individual action loss L_{ind} . The individual action class of an actor who belongs to a group is regarded as the group activity class of the group, and the action class of an outlier is no activity class, denoted by \emptyset .

Total loss. Our model is trained with four losses simultaneously in an end-to-end manner. Specifically, the total training objective of our proposed model is a linear combination of the four losses as follows:

$$L = L_{\text{ind}} + \sum_i L_{\text{group}} + \lambda_m \sum_i L_{\text{mem}} + \lambda_c L_{\text{con}}. \quad (10)$$

5. Experiments

5.1. Implementation Details

Hyperparameters. We use an ImageNet pretrained ResNet-18 as a backbone network. Ground-truth actor tracklets are used to extract actor features with 256 channels by applying RoIAlign with crop size 5×5 . For the Grouping Transformer, we stack 6 Transformer layers with 4 attention heads for Café and JRDB-Act, 3 Transformer layers with 8 attention heads for Social-CAD. The number of group tokens K is set to 12 for Café and JRDB-Act, 10 for Social-CAD.

Training. We sample T frames using the segment-based sampling [43], where T is 5, 1, and 2 for Café, Social-CAD, and JRDB-Act, respectively. We train our model with Adam optimizer [24] with $\beta_1 = 0.9$, $\beta_2 = 0.999$, and $\epsilon = 1e-8$ for 30 epochs. Learning rate is initially set to $1e-5$ with linear warmup to $1e-4$ for 5 epochs, and linearly decayed for remaining epochs. Mini-batch size is set to 16. Loss coefficients are set to $\lambda_m = 5.0$, and $\lambda_c = 2.0$. For the group consistency loss, τ is set to 0.2.

5.2. Comparison with the State of the Art

Compared methods. We compare our method with three clustering-based methods [11, 12, 45] and one Transformer-based method [41]. Since most of GAD methods do not provide the official source code, we try our best to implement the previous work with necessary modifications for dealing with different problem settings, in particular the existence of outliers in Café.

- **ARG** [45]: ARG utilizes graph convolutional networks [25] to model relations between actors in terms of position and appearance similarity. We apply spectral clustering [33] on a relation graph to divide actors into multiple groups.

Method	# Token (# Cluster)	Inference time (s)	Split by view			Split by place		
			Group mAP _{1.0}	Group mAP _{0.5}	Outlier mIoU	Group mAP _{1.0}	Group mAP _{0.5}	Outlier mIoU
ARG [45]	4	0.22	11.03	34.50	56.61	6.87	28.44	46.72
	5	0.26	5.46	30.34	58.89	5.79	24.25	49.25
	6	0.28	1.27	27.69	60.41	2.59	22.33	51.00
	# G + # O	0.30	2.64	28.98	58.21	2.29	22.33	50.01
Joint [11]	4	0.23	13.86	34.68	53.67	6.69	27.76	49.50
	5	0.25	14.05	36.08	60.09	8.39	26.26	55.95
	6	0.28	5.94	33.14	60.63	5.11	24.55	56.94
	# G + # O	0.32	4.54	31.24	59.78	2.87	21.35	56.68
JRDB-base [12]	4	0.23	15.43	34.81	60.43	9.42	25.75	48.00
	5	0.25	13.26	37.40	63.91	9.42	26.19	51.30
	6	0.28	6.77	35.22	63.85	6.37	26.23	51.53
	# G + # O	0.32	4.49	34.40	61.46	3.15	25.80	49.71
HGC [41]	12	0.10	5.18	23.02	57.23	3.50	17.92	57.42
	24	0.10	5.60	21.44	54.57	3.00	14.48	53.64
	50	0.10	6.55	26.29	56.84	3.47	18.46	52.56
	100	0.10	3.63	15.42	54.59	3.07	19.97	56.80
Ours	4	0.10	16.02	40.22	64.06	8.97	27.33	62.35
	8	0.10	<u>18.10</u>	37.51	<u>65.49</u>	<u>9.79</u>	<u>29.23</u>	63.93
	12	0.10	18.84	<u>37.53</u>	67.64	10.85	30.90	<u>63.84</u>
	16	0.10	15.03	37.03	65.31	7.57	25.08	58.66

Table 2. Quantitative results on Café. The second column means the number of tokens for Transformer-based model and the number of clusters for clustering-based models. # G and # O indicates the true number of groups and that of outliers in each video clip, respectively. The third column is the wall-clock inference time for a single video clip measured on a Titan XP GPU. The subscripts of Group mAP mean Group IoU thresholds (θ in Sec. 3.4). We mark the best and the second-best performance in **bold** and underline, respectively.

- *Joint* [11] and *JRDB-base* [12]: These models utilize GNNs to model relations between actors, and train actor representations to partition graphs by adopting a graph edge loss. JRDB-base further adopts geometric features. Then, spectral clustering [33] is applied on the graph.

- *HGC* [41]: Similar to our method, HGC employs the Transformer attention mechanism for GAD. However, unlike our method, HGC identifies group members by point matching between groups and actors on the 2D coordinate space. For a fair comparison, we utilize ground-truth actor tracklets to obtain actor features for HGC.

Café dataset. For a fair comparison, we use ImageNet pre-trained ResNet-18 as the backbone and apply distance mask for all the methods including ours. We test every model on two different dataset splits as explained in Sec. 3.2: *split by view* and *split by place*. Table 2 summarizes the results. Our model outperforms all the other methods by substantial margins on both splits in terms of both Group mAP and Outlier mIoU. Note that the performance of clustering-based methods largely depends on the number of clusters, which is hard to determine or predict when there are outliers in a video clip. On the other hand, our model is less sensitive to the number of group tokens, 12 tokens showed the best performance on both settings though. Our model outperforms HGC, demonstrating the effectiveness of our group-actor matching in an embedding space, as opposed to the point matching strategy used in HGC. We also conduct ex-

Method	Backbone	# frames	Social Accuracy
ARG [45]	Inception-v3	17	49.0
Joint [11]	I3D	17	69.0
Ours	ResNet-18	1	69.2

Table 3. Quantitative results on Social-CAD.

Method	G1 AP	G2 AP	G3 AP	G4 AP	G5 ⁺ AP	mAP
SHGD [28]	3.1	25.0	17.5	45.6	25.2	23.3
Joint [11]	8.0	29.3	37.5	65.4	67.0	41.4
PAR [17]	52.0	59.2	46.7	46.6	31.1	47.1
JRDB-base [12]	81.4	64.8	49.1	63.2	37.2	59.2
Ours	70.1	56.3	50.4	71.7	50.8	59.8

Table 4. Quantitative results on JRDB-Act validation-set using ground-truth bounding boxes.

periments in a detection-based setting for all methods, and the results can be found in Sec. B.3 of the appendix.

Social-CAD dataset. Results on Social-CAD are summarized in Table 3. Our method surpasses the previous methods by leveraging ResNet-18 with a single input frame as backbone, which is significantly lighter than the I3D backbone [4] taking 17 frames as input in the previous work.

JRDB-Act dataset. Table 4 presents results on JRDB-Act val set, where our model achieved the best. Note that our model with the ResNet-18 backbone outperforms JRDB-base with the substantially heavier I3D backbone. In particular, our model demonstrates outstanding performance

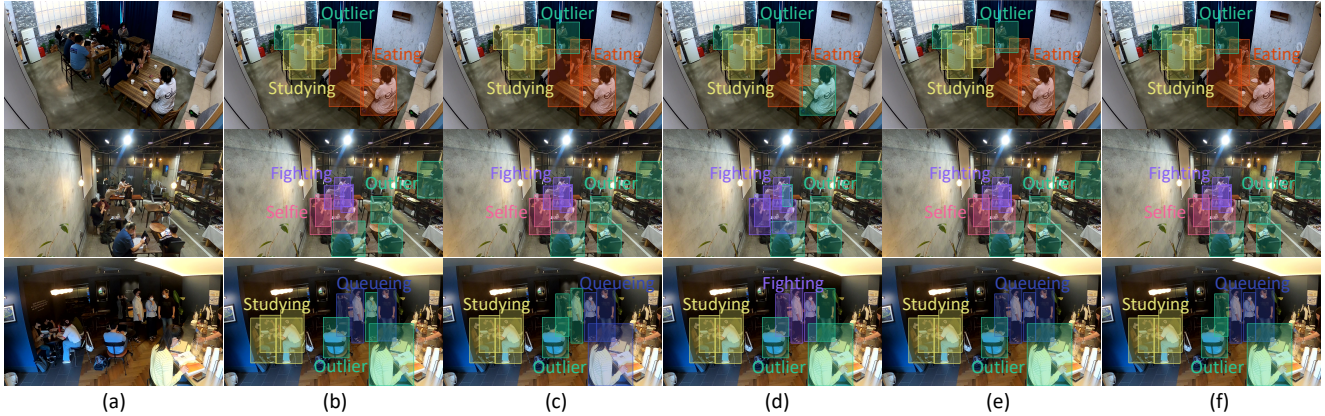


Figure 4. Qualitative results on Café test-set, *split by view* setting. Boxes with the same color belong to the same group. (a) Input frame. (b) Prediction of Joint. (c) Prediction of JRDB-base. (d) Prediction of HGC. (e) Prediction of our model. (f) Ground-truth. More qualitative results can be found in the appendix.

Method	Group mAP _{1.0}	Outlier mIoU
Ours	18.84	67.64
w/o self-attention	13.53 (-5.31)	65.62
w/o cross-attention	13.12 (-5.72)	64.19
w/o grouping-attention	12.92 (-5.92)	64.65

Table 5. Ablation on the attention layers of the Grouping Transformer.

when the group size is larger than 2.

5.3. Ablation Studies

We also verify the effectiveness of our proposed model by ablation studies on Café in the *split by view* setting.

Effects of the attention layers. Table 5 summarizes the effects of multi-head attention layers in Grouping Transformer. Note that self-attention in this table stands for both multi-head self-attention layers that captures relationship between actors and those between groups, cross-attention means multi-head cross-attention layers that actor features attends frame-level features to capture contextual information, and grouping-attention refers to the layers that group tokens attends actor features to form group representation. The results demonstrate that all three attention layers contribute to the performance.

Effects of the distance mask. We investigate the efficacy of utilizing the distance mask. Distance mask inhibits attention between a pair of actors whose distance is greater than the distance threshold μ . As shown in Table 6, applying distance mask between actors is effective in most cases but too small threshold, 0.1 in this table, degrades the performance. It is because actors can interact only with nearby actors at small distance threshold, which might mask the interaction between actors of the same group. Distance threshold of 0.2 reaches the best result while degrades at 0.3.

Effects of the proposed loss function. Table 7 shows the

Distance threshold (μ)	Group mAP _{1.0}	Outlier mIoU
0.1	14.46	62.75
0.2	18.84	67.64
0.3	15.09	63.49
No threshold	14.96	67.03

Table 6. Effects of the distance mask threshold.

L_{con}	Group mAP _{1.0}	Outlier mIoU
X	15.06	63.35
✓	18.84	67.64

Table 7. Effects of the group consistency loss.

effectiveness of the group consistency loss, which improves Group mAP by a substantial margin.

5.4. Qualitative Analysis

Fig. 4 visualizes the predictions of Joint, JRDB-base, HGC, and our model. The results show that our model is able to localize multiple groups and predict their activity classes at the same time, and more reliably than the others, even in challenging crowd scenes with a lot of outliers.

6. Conclusion

In this paper, we have introduced a new large-scale benchmark, dubbed Café, and a new model based on Transformer to present a direction towards more practical GAD. As Café exhibits multiple non-singleton groups per clip and provides rich annotations of actor bounding boxes, track IDs, group configurations, and group activity labels, it can serve as a new, practical, and challenging benchmark for GAD. Also, the proposed model can deal with a varying number of groups as well as predicting members of each group and its activity class. Our model outperformed prior arts on three benchmarks including Café.

Acknowledgements

This work was supported by the NRF grant and the IITP grant funded by Ministry of Science and ICT, Korea (NRF-2021R1A2C3012728, IITP-2020-0-00842, IITP-2019-0-01906 Artificial Intelligence Graduate School Program-POSTECH).

References

- [1] Sina Mokhtarzadeh Azar, Mina Ghadimi Atigh, Ahmad Nickabadi, and Alexandre Alahi. Convolutional relational machine for group activity recognition. In *Proc. IEEE Conference on Computer Vision and Pattern Recognition (CVPR)*, pages 7892–7901, 2019. [1](#)
- [2] Timur Bagautdinov, Alexandre Alahi, François Fleuret, Pascal Fua, and Silvio Savarese. Social scene understanding: End-to-end multi-person action localization and collective activity recognition. In *Proc. IEEE Conference on Computer Vision and Pattern Recognition (CVPR)*, pages 4315–4324, 2017. [2](#)
- [3] Nicolas Carion, Francisco Massa, Gabriel Synnaeve, Nicolas Usunier, Alexander Kirillov, and Sergey Zagoruyko. End-to-end object detection with transformers. In *Proc. European Conference on Computer Vision (ECCV)*, pages 213–229. Springer, 2020. [5](#)
- [4] Joao Carreira and Andrew Zisserman. Quo vadis, action recognition? a new model and the kinetics dataset. In *Proc. IEEE Conference on Computer Vision and Pattern Recognition (CVPR)*, 2017. [7](#)
- [5] Wongun Choi, Khuram Shahid, and Silvio Savarese. What are they doing?: Collective activity classification using spatio-temporal relationship among people. In *Proc. IEEE International Conference on Computer Vision (ICCV) Workshops*, pages 1282–1289. IEEE, 2009. [1](#), [2](#), [3](#), [12](#)
- [6] Wongun Choi, Yu-Wei Chao, Caroline Pantofaru, and Silvio Savarese. Discovering groups of people in images. In *Proc. European Conference on Computer Vision (ECCV)*, pages 417–433. Springer, 2014. [4](#)
- [7] Patrick Dendorfer, Aljosa Osep, Anton Milan, Konrad Schindler, Daniel Cremers, Ian Reid, Stefan Roth, and Laura Leal-Taixé. Motchallenge: A benchmark for single-camera multiple target tracking. *International Journal of Computer Vision (IJCV)*, 129(4):845–881, 2021. [3](#)
- [8] Jia Deng, Wei Dong, Richard Socher, Li-Jia Li, Kai Li, and Li Fei-Fei. Imagenet: A large-scale hierarchical image database. In *Proc. IEEE Conference on Computer Vision and Pattern Recognition (CVPR)*, pages 248–255, 2009. [5](#)
- [9] Zhiwei Deng, Arash Vahdat, Hexiang Hu, and Greg Mori. Structure inference machines: Recurrent neural networks for analyzing relations in group activity recognition. In *Proc. IEEE Conference on Computer Vision and Pattern Recognition (CVPR)*, pages 4772–4781, 2016. [2](#)
- [10] Alexey Dosovitskiy, Lucas Beyer, Alexander Kolesnikov, Dirk Weissenborn, Xiaohua Zhai, Thomas Unterthiner, Mostafa Dehghani, Matthias Minderer, Georg Heigold, Sylvain Gelly, Jakob Uszkoreit, and Neil Houlsby. An image is worth 16x16 words: Transformers for image recognition at scale. In *Proc. International Conference on Learning Representations (ICLR)*, 2021. [2](#), [3](#), [4](#)
- [11] Mahsa Ehsanpour, Alireza Abedin, Fatemeh Saleh, Javen Shi, Ian Reid, and Hamid Rezaatofghi. Joint learning of social groups, individuals action and sub-group activities in videos. In *Proc. European Conference on Computer Vision (ECCV)*, pages 177–195. Springer, 2020. [1](#), [2](#), [3](#), [4](#), [5](#), [6](#), [7](#), [12](#), [14](#), [15](#)
- [12] Mahsa Ehsanpour, Fatemeh Saleh, Silvio Savarese, Ian Reid, and Hamid Rezaatofghi. Jrdb-act: A large-scale dataset for spatio-temporal action, social group and activity detection. In *Proc. IEEE Conference on Computer Vision and Pattern Recognition (CVPR)*, pages 20983–20992, 2022. [1](#), [2](#), [3](#), [4](#), [5](#), [6](#), [7](#), [12](#), [14](#), [15](#)
- [13] Andreas Ess, Bastian Leibe, Konrad Schindler, and Luc Van Gool. A mobile vision system for robust multi-person tracking. In *Proc. IEEE Conference on Computer Vision and Pattern Recognition (CVPR)*, pages 1–8. IEEE, 2008. [3](#)
- [14] Mark Everingham, SM Ali Eslami, Luc Van Gool, Christopher KI Williams, John Winn, and Andrew Zisserman. The pascal visual object classes challenge: A retrospective. *International Journal of Computer Vision (IJCV)*, 111:98–136, 2015. [4](#)
- [15] Kirill Gavriluk, Ryan Sanford, Mehrsan Javan, and Cees GM Snoek. Actor-transformers for group activity recognition. In *Proc. IEEE Conference on Computer Vision and Pattern Recognition (CVPR)*, pages 839–848, 2020. [1](#), [3](#), [5](#)
- [16] Zheng Ge, Songtao Liu, Feng Wang, Zeming Li, and Jian Sun. YOLOX: Exceeding yolo series in 2021. *arXiv preprint arXiv:2107.08430*, 2021. [3](#)
- [17] Ruize Han, Haomin Yan, Jiacheng Li, Songmiao Wang, Wei Feng, and Song Wang. Panoramic human activity recognition. In *Proc. European Conference on Computer Vision (ECCV)*, pages 244–261. Springer, 2022. [7](#)
- [18] Kaiming He, Xiangyu Zhang, Shaoqing Ren, and Jian Sun. Deep residual learning for image recognition. In *Proc. IEEE Conference on Computer Vision and Pattern Recognition (CVPR)*, pages 770–778, 2016. [5](#)
- [19] Kaiming He, Georgia Gkioxari, Piotr Dollár, and Ross Girshick. Mask r-cnn. In *Proc. IEEE International Conference on Computer Vision (ICCV)*, pages 2961–2969, 2017. [5](#)
- [20] Guyue Hu, Bo Cui, Yuan He, and Shan Yu. Progressive relation learning for group activity recognition. In *Proc. IEEE Conference on Computer Vision and Pattern Recognition (CVPR)*, pages 980–989, 2020. [3](#)
- [21] Mostafa S Ibrahim and Greg Mori. Hierarchical relational networks for group activity recognition and retrieval. In *Proc. European Conference on Computer Vision (ECCV)*, pages 721–736, 2018. [2](#)
- [22] Mostafa S Ibrahim, Srikanth Muralidharan, Zhiwei Deng, Arash Vahdat, and Greg Mori. A hierarchical deep temporal model for group activity recognition. In *Proc. IEEE Conference on Computer Vision and Pattern Recognition (CVPR)*, pages 1971–1980, 2016. [2](#), [12](#)
- [23] Dongkeun Kim, Jinsung Lee, Minsu Cho, and Suha Kwak. Detector-free weakly supervised group activity recognition.

- In *Proc. IEEE Conference on Computer Vision and Pattern Recognition (CVPR)*, pages 20083–20093, 2022. 1, 3
- [24] Diederik P. Kingma and Jimmy Ba. Adam: A method for stochastic optimization. In *Proc. International Conference on Learning Representations (ICLR)*, 2015. 6
- [25] Thomas N Kipf and Max Welling. Semi-supervised classification with graph convolutional networks. *Proc. International Conference on Learning Representations (ICLR)*, 2017. 6
- [26] Harold W Kuhn. The hungarian method for the assignment problem. *Naval research logistics quarterly*, 2(1-2):83–97, 1955. 5
- [27] Feng Li, Hao Zhang, Shilong Liu, Jian Guo, Lionel M Ni, and Lei Zhang. Dn-detr: Accelerate detr training by introducing query denoising. In *Proc. IEEE Conference on Computer Vision and Pattern Recognition (CVPR)*, pages 13619–13627, 2022. 6
- [28] Jiacheng Li, Ruize Han, Haomin Yan, Zekun Qian, Wei Feng, and Song Wang. Self-supervised social relation representation for human group detection. In *Proc. European Conference on Computer Vision (ECCV)*, pages 142–159. Springer, 2022. 7
- [29] Shuaicheng Li, Qianggang Cao, Lingbo Liu, Kunlin Yang, Shinan Liu, Jun Hou, and Shuai Yi. Groupformer: Group activity recognition with clustered spatial-temporal transformer. In *Proc. IEEE International Conference on Computer Vision (ICCV)*, pages 13668–13677, 2021. 1, 3, 5
- [30] Wei Li, Tianzhao Yang, Xiao Wu, Xian-Jun Du, and Jian-Jun Qiao. Learning action-guided spatio-temporal transformer for group activity recognition. In *Proceedings of the 30th ACM International Conference on Multimedia*, pages 2051–2060, 2022. 3
- [31] Xin Li and Mooi Choo Chuah. Sbgar: Semantics based group activity recognition. In *Proc. IEEE International Conference on Computer Vision (ICCV)*, pages 2876–2885, 2017. 2
- [32] Roberto Martin-Martin, Mihir Patel, Hamid Rezaatofghi, Abhijeet Sheno, JunYoung Gwak, Eric Frankel, Amir Sadeghian, and Silvio Savarese. Jrdb: A dataset and benchmark of egocentric robot visual perception of humans in built environments. *IEEE Transactions on Pattern Analysis and Machine Intelligence (TPAMI)*, 2021. 1, 3
- [33] Andrew Ng, Michael Jordan, and Yair Weiss. On spectral clustering: Analysis and an algorithm. *Proc. Neural Information Processing Systems (NeurIPS)*, 14, 2001. 3, 6, 7
- [34] Aaron van den Oord, Yazhe Li, and Oriol Vinyals. Representation learning with contrastive predictive coding. *arXiv preprint arXiv:1807.03748*, 2018. 6
- [35] Rizard Renanda Adhi Pramono, Yie Tarng Chen, and Wen Hsien Fang. Empowering relational network by self-attention augmented conditional random fields for group activity recognition. In *Proc. European Conference on Computer Vision (ECCV)*, pages 71–90. Springer, 2020. 1, 3
- [36] Mengshi Qi, Jie Qin, Annan Li, Yunhong Wang, Jiebo Luo, and Luc Van Gool. stagnet: An attentive semantic rnn for group activity recognition. In *Proc. European Conference on Computer Vision (ECCV)*, pages 101–117, 2018. 2
- [37] Linbo Qing, Lindong Li, Shengyu Xu, Yibo Huang, Mei Liu, Rulong Jin, Bo Liu, Tong Niu, Hongqian Wen, Yuchen Wang, et al. Public life in public space (plps): A multi-task, multi-group video dataset for public life research. In *Proc. IEEE International Conference on Computer Vision (ICCV) Workshops*, pages 3618–3627, 2021. 2
- [38] Hamid Rezaatofghi, Nathan Tsoi, JunYoung Gwak, Amir Sadeghian, Ian Reid, and Silvio Savarese. Generalized intersection over union: A metric and a loss for bounding box regression. In *Proc. IEEE Conference on Computer Vision and Pattern Recognition (CVPR)*, pages 658–666, 2019. 14
- [39] Shuai Shao, Zijian Zhao, Boxun Li, Tete Xiao, Gang Yu, Xiangyu Zhang, and Jian Sun. Crowdhuman: A benchmark for detecting human in a crowd. *arXiv preprint arXiv:1805.00123*, 2018. 3
- [40] Tianmin Shu, Sinisa Todorovic, and Song-Chun Zhu. Cern: confidence-energy recurrent network for group activity recognition. In *Proc. IEEE Conference on Computer Vision and Pattern Recognition (CVPR)*, pages 5523–5531, 2017. 2
- [41] Masato Tamura, Rahul Vishwakarma, and Ravigopal Venelakanti. Hunting group clues with transformers for social group activity recognition. In *Proc. European Conference on Computer Vision (ECCV)*, 2022. 1, 3, 6, 7, 14, 15
- [42] Ashish Vaswani, Noam Shazeer, Niki Parmar, Jakob Uszkoreit, Llion Jones, Aidan N Gomez, Łukasz Kaiser, and Illia Polosukhin. Attention is all you need. In *Proc. Neural Information Processing Systems (NeurIPS)*, pages 5998–6008, 2017. 2, 3, 4
- [43] Limin Wang, Yuanjun Xiong, Zhe Wang, Yu Qiao, Dahua Lin, Xiaoou Tang, and Luc Van Gool. Temporal segment networks: Towards good practices for deep action recognition. In *Proc. European Conference on Computer Vision (ECCV)*, pages 20–36. Springer, 2016. 6
- [44] Minsi Wang, Bingbing Ni, and Xiaokang Yang. Recurrent modeling of interaction context for collective activity recognition. In *Proc. IEEE Conference on Computer Vision and Pattern Recognition (CVPR)*, pages 3048–3056, 2017. 2
- [45] Jianchao Wu, Limin Wang, Li Wang, Jie Guo, and Gangshan Wu. Learning actor relation graphs for group activity recognition. In *Proc. IEEE Conference on Computer Vision and Pattern Recognition (CVPR)*, pages 9964–9974, 2019. 1, 3, 5, 6, 7, 14
- [46] Rui Yan, Jinhui Tang, Xiangbo Shu, Zechao Li, and Qi Tian. Participation-contributed temporal dynamic model for group activity recognition. In *Proc. ACM Multimedia Conference (ACMMM)*, pages 1292–1300, 2018. 2
- [47] Rui Yan, Lingxi Xie, Jinhui Tang, Xiangbo Shu, and Qi Tian. Hgcin: hierarchical graph-based cross inference network for group activity recognition. *IEEE Transactions on Pattern Analysis and Machine Intelligence (TPAMI)*, 2020. 3
- [48] Rui Yan, Lingxi Xie, Jinhui Tang, Xiangbo Shu, and Qi Tian. Social adaptive module for weakly-supervised group activity recognition. In *Proc. European Conference on Computer Vision (ECCV)*, pages 208–224. Springer, 2020. 2, 12
- [49] Hangjie Yuan and Dong Ni. Learning visual context for group activity recognition. In *Proc. AAAI Conference on Artificial Intelligence (AAAI)*, pages 3261–3269, 2021. 3, 5

- [50] Hangjie Yuan, Dong Ni, and Mang Wang. Spatio-temporal dynamic inference network for group activity recognition. In *Proc. IEEE International Conference on Computer Vision (ICCV)*, pages 7476–7485, 2021. [1](#), [3](#)
- [51] Lihi Zelnik-Manor and Pietro Perona. Self-tuning spectral clustering. *Proc. Neural Information Processing Systems (NeurIPS)*, 17, 2004. [3](#)
- [52] Shanshan Zhang, Rodrigo Benenson, and Bernt Schiele. Citypersons: A diverse dataset for pedestrian detection. In *Proc. IEEE Conference on Computer Vision and Pattern Recognition (CVPR)*, pages 3213–3221, 2017. [3](#)
- [53] Yifu Zhang, Peize Sun, Yi Jiang, Dongdong Yu, Zehuan Yuan, Ping Luo, Wenyu Liu, and Xinggang Wang. Byte-track: Multi-object tracking by associating every detection box. In *Proc. European Conference on Computer Vision (ECCV)*, 2022. [3](#), [14](#)
- [54] Xizhou Zhu, Weijie Su, Lewei Lu, Bin Li, Xiaogang Wang, and Jifeng Dai. Deformable detr: Deformable transformers for end-to-end object detection. In *Proc. International Conference on Learning Representations (ICLR)*, 2021. [3](#)

Appendix

This appendix presents contents omitted in the main paper due to the page limit. Sec. A presents more details of our proposed Café dataset. Further analysis on the quantitative results, experiments in detection-based setting, more qualitative results are given in Sec. B.1, Sec. B.2, and Sec. B.3 respectively.

A. More Detailed Information of Café

A.1. Data Acquisition

To construct practical group activity detection (GAD) dataset, we recruit participants, direct their actions, and record with cameras. We take videos at six different cafes, installing cameras at four different locations within each cafe to capture the same scene from four distinct viewpoints. Videos of Café are recorded with four RGB cameras at 1920×1080 resolution, then are cut into clips at 6-seconds intervals. Members of each group and clothes of participants change periodically to prevent monotonous grouping patterns. Note that we obtain informed consent of participants to release the dataset publicly.

In each video clip, actors are divided into multiple groups and outliers. Members of each group are asked to perform one of predefined group activities: *queueing*, *ordering*, *eating*, *working*, *fighting*, and *taking selfie*. On the other hand, outliers who do not belong to any group, perform arbitrary action (e.g. look at a smart phone or work on a laptop). Note that actors who are close together but do not interact with any group members are also considered as outliers. Therefore, localizing group members necessitates understanding the properties of individual actors and their relationship as well as their spatial proximity.

Fig. S1 provides qualitative examples of videos in Café for each place along with annotations including bounding boxes of humans, group configurations, and group activity labels. Each place of Café show different characteristics such as different camera viewpoints, group configurations, and light condition. Additionally, one among six places of Café in part includes outdoor scenes, which diversify the scene variety of Café. Examples of Café raw videos can be found in the project page (<https://cvlab.postech.ac.kr/research/CAFE>). All video frames and annotations will be open to public for the research community.

A.2. Additional Dataset Statistics

Additional statistics of *split by place* and *split by view* training-validation-test split are shown in Table S1 and Table S2, respectively. The number of clips, frames, boxes, and groups are evenly distributed across each place and camera view. The average number of frames per clip is 33.36, the average number of boxes per frame is 10.5, and

Place	# Clips	# Frames	# Boxes	# Groups
Training				
A	1851	59246	620194	2628
B	1628	55603	555517	2455
C	1616	55369	601309	3117
D	1614	55194	576952	2630
Validation				
E	1423	48291	510868	2224
Test				
F	2165	69756	742458	2917

Table S1. Statistics of Café *split by place* training-validation-test split. # represents “the number of”. Example videos and annotations of each place are illustrated in Fig. S1.

View	# Clips	# Frames	# Boxes	# Groups
Training				
α	2574	85901	898486	3940
β	2572	85777	916590	4056
Validation				
γ	2576	86049	920179	4063
Test				
δ	2575	85732	872043	3912

Table S2. Statistics of Café *split by view* training-validation-test split. # represents “the number of”. There are 4 different camera viewpoints for each place, it is named α , β , γ , and δ , respectively.

the average number of groups per clip is 1.55. FPS of original videos is 29.9 on average.

A.3. About Group Activity Class Definition

Having only six group activity classes might seem limited, but we choose the current group activity classes for the following reasons. (1) The variety of group activity classes is inherently limited. Even in existing datasets [5, 11, 12, 22, 48], the number of group activity classes has been relatively fewer compared to classes in individual action classes. For instance, in the JRDB-Act dataset, there were only three person-to-person activity classes while total 26 action classes. (2) Although classes such as *eating* and *working* can be done individually, our definition of group activity involves actions performed collectively by a group of people. This aligns with the definition of the existing GAR and GAD datasets [11, 12]. (3) When taking the videos, actors were encouraged to wear masks except while eating, to prevent COVID-19 infection, making it challenging to define group activity classes such as *talking*.

Time →



Figure S1. Qualitative examples of videos in Café for each place along with annotations. Each color represents different groups and all outliers are marked with red color.

B. More Experimental Results

B.1. Analysis of Activity Classification

Fig. S2 shows the confusion matrix on two different dataset splits of Café: *split by view* and *split by place*. Note that these confusion matrices are computed based on predicted group and ground-truth group pairs with Group IoU greater than or equal to 0.5. Due to the class imbalance problem, our method shows poor performance on *queueing* and *ordering* class which are the least frequent and the second least frequent group activity class on Café. For these classes, most of the activities of the groups are classified as outliers. In the future, this problem can be handled by applying the inverse of class frequency as a weight for the group activity classifier or adopting focal loss. In both dataset splits, the most confusing group activity classes are *queueing* versus *ordering* which frequently co-occur.

B.2. Detection-based Setting on Café

To show the effectiveness of our proposed method in realistic situation, we replace the ground-truth actor tracklets with the predicted actor tracklets which are obtained by utilizing off-the-shelf multi-object tracker [53].

Tracklet Matching. Similar to group matching explained in Sec. 4.2 of the main paper, we need another bipartite matching between ground-truth tracklets and predicted tracklets to train the model in detection-based setting. Among all possible combinations of N ground-truth tracklets and M predicted tracklets ($M \geq N$ in our case), Hungarian algorithm finds the permutation with the lowest matching cost:

$$\hat{\sigma} = \arg \min_{\sigma \in \mathfrak{S}_M} \sum_i^N C_{i, \sigma(i)}, \quad (11)$$

where the matching cost of the ground-truth tracklet i and the predicted tracklet $\sigma(i)$ is defined as

$$C_{i, \sigma(i)} = \sum_{t=1}^T (\lambda_{L1} \|b_{i,t} - \hat{b}_{\sigma(i),t}\|_1 + \lambda_{giou} L_{giou}(b_{i,t}, \hat{b}_{\sigma(i),t})), \quad (12)$$

where $b_{i,t}$ is the bounding box of ground-truth tracklet i at frame t , $\hat{b}_{\sigma(i),t}$ is the bounding box of predicted tracklet $\sigma(i)$ at frame t , T is the number of frames for each video clip, L_{giou} is the generalized IoU loss [38], $\lambda_{L1} = 5.0$, and $\lambda_{giou} = 2.0$.

Evaluation. To measure the performance in the detection-based setting, we need identity matching between the predicted tracklets and the ground-truth tracklets. We follow standard box matching strategy used in object detection, utilize the mean IoU over T frames as the IoU threshold and the mean confidence over T frames as the detection confidence score of the predicted tracklet. We adopt IoU threshold of 0.5 following previous methods [11, 12].

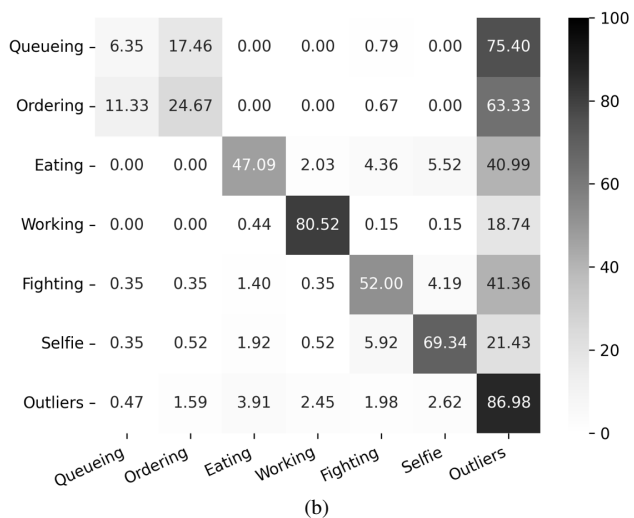
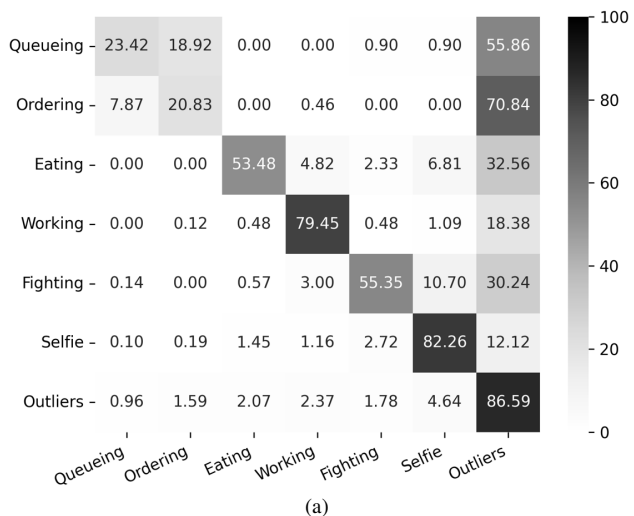


Figure S2. The confusion matrix on Café: (a) *split by view* setting, (b) *split by place* setting.

Comparison with the Previous Work. We implement previous GAR and GAD methods [11, 41, 45] as explained in Sec. 5.2 of the main paper and test our proposed model and other methods on two different dataset splits: *split by view* and *split by place*. We adopt three evaluation metrics: Group $mAP_{1.0}$, Group $mAP_{0.5}$, and Outlier mIoU. Group $mAP_{1.0}$ is the primary measure for GAD, a predicted group is considered as true positive only when including correct members only. Group $mAP_{0.5}$ allows small mistakes on group localization, and Outlier mIoU measures outlier detection performance. Table S3 summarizes the results of detection-based setting on Café. The proposed model outperforms other methods on both dataset splits. Although JRDB-base [12] is comparable to our model on *split by place* setting in terms of Group $mAP_{1.0}$, our model largely outperforms in terms of Group $mAP_{0.5}$ and Outlier

Method	Split by view			Split by place		
	Group mAP _{1.0}	Group mAP _{0.5}	Outlier mIoU	Group mAP _{1.0}	Group mAP _{0.5}	Outlier mIoU
ARG	7.92	29.83	48.82	6.70	<u>26.27</u>	48.32
Joint	9.14	31.83	42.93	6.08	18.43	2.83
JRDB-base	<u>12.63</u>	<u>35.53</u>	31.85	<u>8.15</u>	22.68	33.03
HGC	6.77	31.08	<u>57.65</u>	4.27	24.97	<u>57.70</u>
Ours	14.36	37.52	63.70	8.29	28.72	59.60

Table S3. Comparison with the previous GAR and GAD models on Café detection-based setting. We mark the best and the second-best performance in **bold** and underline, respectively.

mIoU. While the performance of most methods including ours drop in detection-based setting when compared to the use of ground-truth actor tracklets, the performance of HGC does not drop as it employs box prediction loss which can be used to refine actor features obtained from incorrect predicted actor tracklets. Nevertheless, our proposed method still outperforms HGC even when evaluated in detection-based setting.

B.3. More Qualitative Results

Fig. S3 visualizes the predictions of Joint [11], JRDB-base [12], HGC [41], and our model. The results show that our model is able to localize multiple groups more reliably than others, such as *fighting* group for second example and *taking selfie* group for third example.

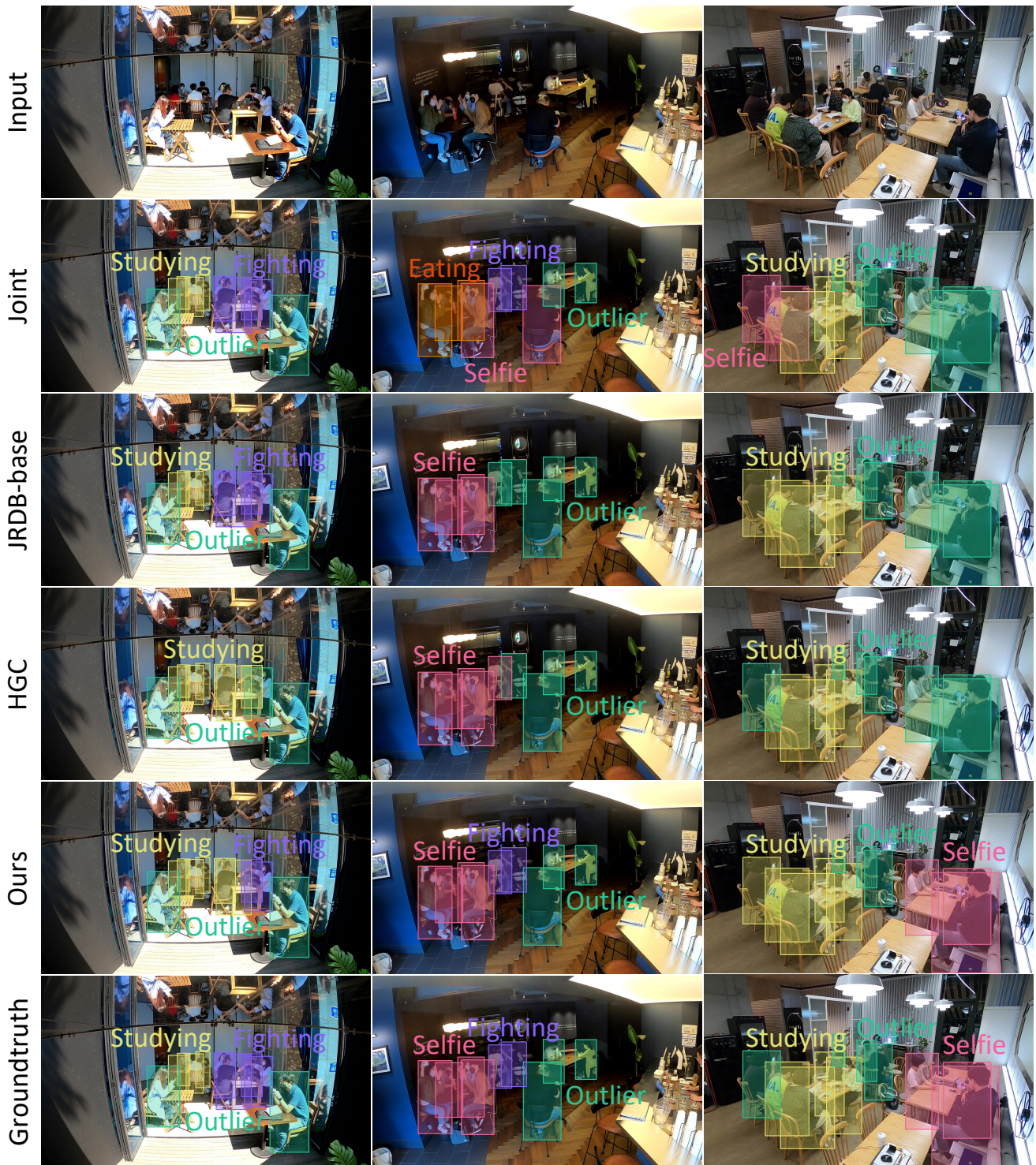


Figure S3. More qualitative results on Café test-set, *split by view setting*. Boxes with the same color belong to the same group.